NASA CR-54932

SECOND QUARTERLY REPORT

RESEARCH & DEVELOPMENT IN CdS PHOTOVOLTAIC CELLS

BY

J. C. Schaefer, E. R. Hill, T. A. Griffin

Prepared For

NATIONAL AERONAUTICS AND SPACE ADMINISTRATION

September 28, 1965 to December 29, 1965

CONTRACT NAS-7631

THE HARSHAW CHEMICAL CO.

N O T I C E

This report was prepared as an account of Government sponsored work. Neither the United States, nor the National Aeronautics and Space Administration (NASA), nor any person acting on behalf of NASA:

A.) Makes any warranty or representation, expressed or implied, with respect to the accuracy, completeness, or usefulness of the information contained in this report, or that the use of any information, apparatus, method, or process disclosed in this report may not infringe privately owned rights; or

B.) Assumes any liabilities with respect to the use of, or for damages resulting from the use of any information, apparatus, method, or process disclosed in this report.

As used above, "person acting on behalf of NASA" includes any employee or contractor of NASA, or employee of such contractor, to the extent that such contractor prepares, disseminates, or provides access to, any information pursuant to his employment or contract with NASA, or his employment with such contractor.

Requests for copies of this report should be referred to:

National Aeronautics and Space Administration
Office of Scientific and Technical Information
Attention: AFSS-A
Washington, D.C. 20546

NASA CR-54932

SECOND QUARTERLY REPORT

RESEARCH AND DEVELOPMENT

IN

CdS PHOTOVOLTAIC FILM CELLS

by

J. C. Schaefer, E. R. Hill, T. A. Griffin

Prepared For

NATIONAL AERONAUTICS AND SPACE ADMINISTRATION

September 28, 1965 to December 29, 1965

Contract NAS 3-7631

Technical Management
NASA Lewis Research Center
Cleveland, Ohio
Space Power Systems Division
Clifford Swartz

Harshaw Chemical Company
Crystal-Solid State Division
1945 E. 97th Street
Cleveland 6, Ohio

FOREWORD

This report was prepared by the Crystal-Solid State Division of The Harshaw Chemical Company. The work has been sponsored by the Space Power Systems Procurement Section of the NASA Lewis Research Center with Dr. A. E. Potter acting as Technical Advisor and Mr. Clifford Swartz acting as Project Manager.

Project direction has been provided by Mr. J. C. Schaefer with Mr. E. R. Hill and Mr. T. A. Griffin acting as principal investigators for the research and development work respectively. The following Harshaw personnel have contributed to this program: B. Keramidas, R. J. Humrick, R. W. Olmsted, D. J. Krus, W. W. Baldauf, N. E. Heyerdahl, P. J. Marn, and C. A. Morano. Dr. N. K. Pope of the Royal Military College of Canada served as consultant.

Abstract

N66-22935

The CdS film cell has been studied with regard to the light absorbing material and the charge separating mechanism. Cells are reported to have been destroyed electrically and returned to original power. Vapor transport studies have continued for CdS but not for Cu_2S. Experiments on collector grids, interface materials, CdS surface treatments, non-aqueous barrier formation solutions and substrate milling, are reported.

Author

Table of Contents

List of Illustrations

List of Tables

Summary

The research on the CdS cell and model has been continued. Studies of the light absorbing material of the cell have shown a change in cell response with increasing temperature while the bandgap decreases about 10^{-3} eV per °K. For energies between about 1.4 and 2.4 eV, the function yield decreases with increasing temperature. At 400°K a step appears at 2.4 eV which does not appear at lower temperatures.

Studies of the charge separating mechanism and the hysteresis evident in the I-V curve has shown the means of literally destroying a cell with a forward bias and returning it to full output with a reverse bias. Power can still be extracted after application of forward bias which has been recognized as a persistent internal polarization.

A silver interface layer between the CdS layer and the metallic substrate appears to be beneficial.

The CdS vapor transport method of forming a film was continued. Film thickness and resistivity can be reasonably controlled by proper mixing of charge, period of transport and temperature of the boat. Thicknesses of 20 μ to 30 μ and resistivities of 10 to 100 ohm-cm are readily produced. The transport rate is affected by the total time of heater useage.

Acid etching of CdS before the formation of the barrier layer is shown to be essential for higher efficiency solar cells.

Vapor transport of Cu_2S has been curtailed because of lack of an indication of immediate benefit toward improved cell efficiency. The work to date has been summarized in this report.

Collector grids formed by electrodeposition have improved

in efficiency but do not show a last-step improvement in power during lamination. Grids can also be applied by pressure and have been so produced. Time will show whether these are satisfactory. This procedure may allow fabrication of cells without any plastic encapsulation or reinforcement.

Chemical and electrochemical milling of substrates after cell fabrication has been demonstrated to be practical. Procedure is reported and discussed.

INTRODUCTION

The cadmium sulfide (CdS) solar cell in its present state of development is composed of a thin evaporated film of CdS on a conductive substrate with a barrier layer formed along the surface of the film. The substrate also serves as a current collector. A grid is affixed to the barrier layer in order to collect the available power. Since the cell is changing rather often a more specific description is not warranted.

Further changes were indicated by the model concept reported at the Photovoltaic Specialist Conference in October at the NASA, Goddard Space Flight Center. Uniform layer thicknesses of CdS and cuprous sulfide (Cu_2S) are desired if a maximum conversion efficiency and power output are to be achieved.

Evaporated CdS films do not provide all of the desired qualities. Experiments to form films by vapor transport have indicated that the desired film thickness, uniformity, freedom from pin holes and cracks, and control of bulk film properties are possible. The application of a uniformly thick vapor transported barrier layer would provide a cell within the concept of the CdS model. Cu_2S can be vapor transported, but at excessive temperatures. Barrier formation by solution dipping or electroplating fails to produce a uniform thickness or continuity.

Vapor transport of CdS may prove to be significant since a low material utilization is inherent in evaporation, whereas, a very high utilization factor is immediately apparent for the vapor transport method. This will be a major consideration in production.

Current collection at the barrier layer has always been a problem. Good collection of current initially and throughout prolonged thermal cycling are the prime objectives. Operating cells with collector grids applied by electroplating have accomplished the objectives. Pressure techniques have also been found to provide a means of attaching grids.

Cell model studies have provided additional data. These studies have been concerned with the light absorbing material and the charge separating mechanism. The cell junction can be changed by applying a forward or reverse bias.

Research on the CdS Model

The two crucial elements of a solar cell are the light absorbing material and the charge separating mechanism. These two areas have been investigated during this quarter.

Light Absorbing Material

The absorption was examined in respect to the temperature dependence of the spectral response of the cell. A chemi-plated 3.5% efficient cell laminated in Mylar was mounted on a small hot plate which was placed at the exit slit of a monochromator. Spectral response was then measured at 200°K, 300°K, and 400°K. The data are shown in Figure 1. The significant features are as follows:

1. At the low energy limit, the change in response is that due to the temperature dependence of the bandgap. That is, the temperature increases, while the bandgap decreases at the rate of about 10^{-3} eV per °K. The slope should also change as the reciprocal of the absolute temperature, but the noise level obscures this small effect.
2. For energies between about 1.4 and 2.4 eV the quantum yield decreases with increasing temperature.
3. At temperatures around 400°K, a step is seen at 2.4 eV which is not present at lower temperatures.

The effects in 2 and 3 can be explained by examination of the chemical reaction which is used to make the cell, which is:

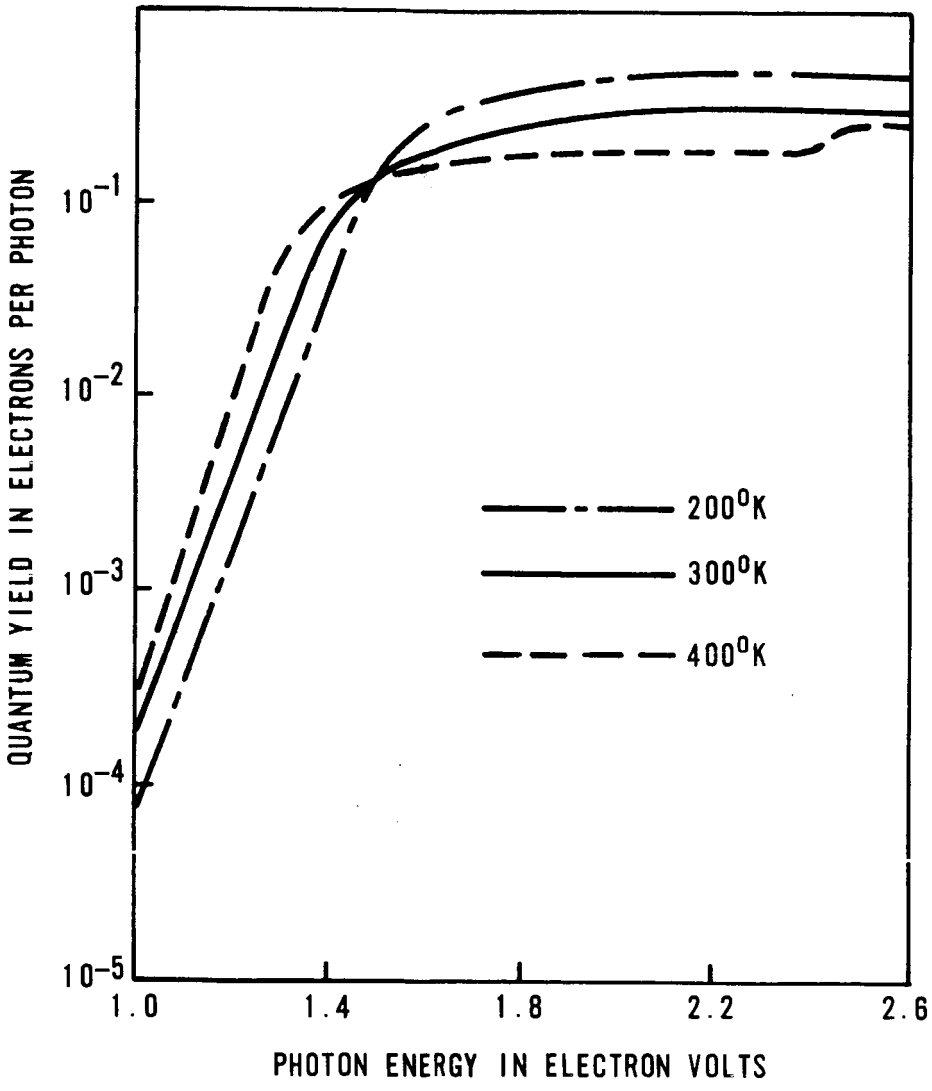

Fig. 1 TEMPERATURE VARIATION OF CdS SOLAR CELL SPECTRAL RESPONSE

$$Cu_2Cl_2 + CdS = Cu_2S + CdCl_2$$

$$F^\circ\ (298^\circ K) = -12\ \frac{k\ cal}{Mole}$$

$$Ln\ \frac{[Cu_2S]\ [CdCl_2]}{[Cu_2Cl_2]\ [CdS]} = \frac{-\Delta F}{RT}$$

If Cu_2S is assumed to be the active material for photons in the range from 1 to 2.4 eV, then the quantum yield will be temperature dependent. As the temperature increases, the right-hand term becomes a smaller number, and the concentration of Cu_2S decreases. Likewise, the CdS concentration in the region of the cell surface increases with increasing temperature, resulting in the step at 2.4 eV at higher temperatures.

The net result of increasing temperature is to cause a decrease in sunlight generated current. The loss in response between 1.4 and 2.4 eV far outweighs the gain due to the decreased bandgap. The change appears to be linear over this temperature range. The open circuit voltage also decreases linearly with temperature, at the rate of above 1 millivolt per °K. These two effects are shown in Figure 2. If the fill factor remains constant, power will vary parabolically with temperature. For small changes in this range the quadratic term is small and a linear function is a close approximation with a coefficient of the sum of the rates of change of voltage and current. This can be expressed analytically as follows:

$$I = I_\circ\ \frac{-dI}{dT}\ T = \text{short circuit current}$$

$$V_\circ = V_\circ\ \frac{-dV}{dT}\ T = \text{open circuit voltage}$$

$$\text{Power} = IV = I_\circ V_\circ - V_\circ \frac{dI}{dT} - I_\circ \frac{dV}{dT}\ T + \frac{dI}{dT}\ \frac{dV}{dT}\ T^2$$

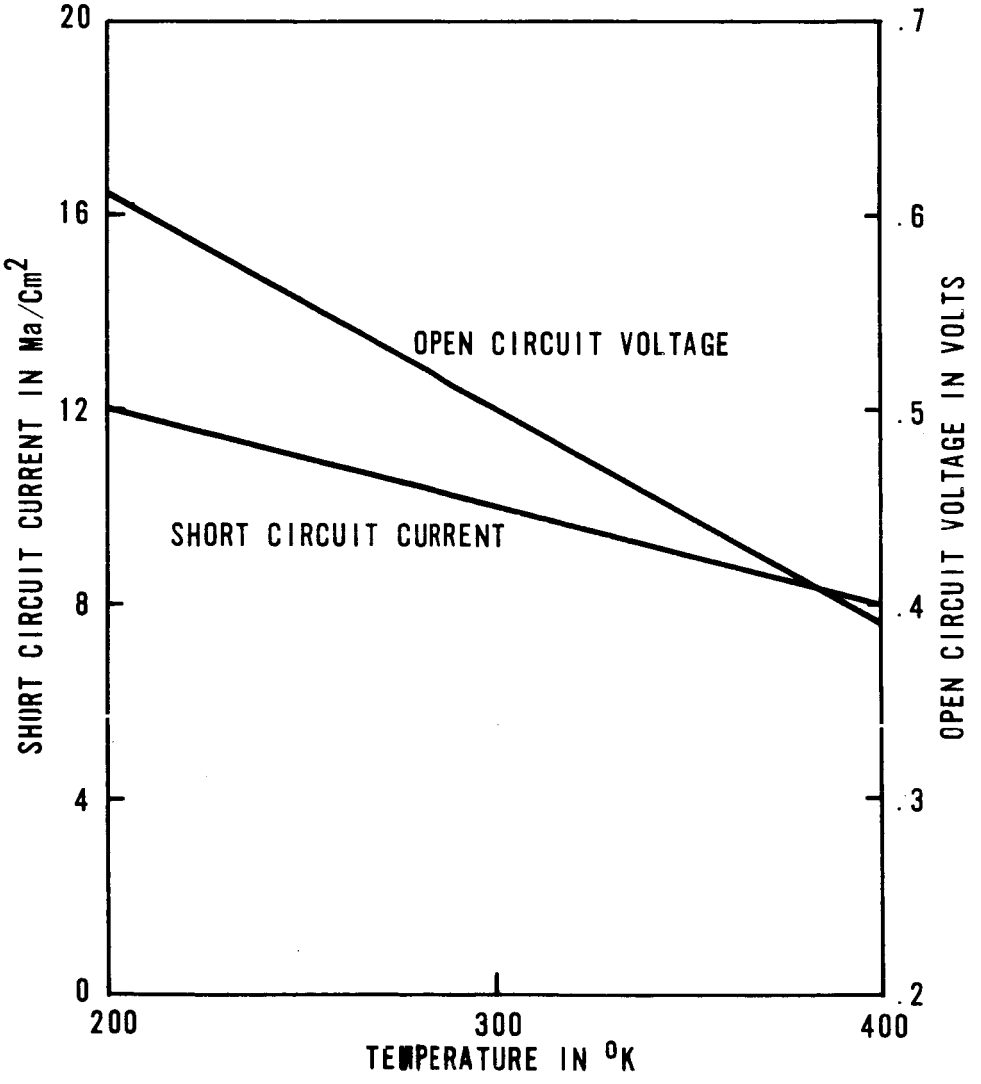

Fig. 2 TEMPERATURE DEPENDENCE OF OPEN CIRCUIT VOLTAGE AND SHORT CIRCUIT CURRENT FOR CdS SOLAR CELL

The last term is small, so

$$P = IV \simeq I_o V_o - V_o \frac{dI}{dT} - I_o \frac{dV}{dT} T$$

$$\frac{dP}{dT} = -V_o \frac{dI}{dT} - I_o \frac{dV}{dT}$$

$$\frac{1}{I_o V_o} \frac{dP}{dT} = -\frac{1}{I_o} \frac{dI}{dT} - \frac{1}{V_o} \frac{dV}{dT}$$

Thus, the fraction change in power is the sum of the fractional changes in current and voltage. Using the data shown in Figure 2, this results in a fraction rate of change of power at room temperature of

$$\frac{1}{P} \frac{dP}{dT} = 4 \times 10^{-3} /^{\circ}K \text{ at } 300^{\circ}K$$

Charge Separating Mechanism and Cell Reversibility

To examine the charge separating mechanism, or the junction, data on I-V curves has been taken. As noted in the first quarterly report, an effect of hysteresis was evident in the I-V curve. When the curve was traced at a finite rate, the ascending and decending branches were separated. It was noticed during the last quarter that the cell could be physically changed by applying forward or reverse bias for a normal cell taken in the dark with a 60 cycle sweep voltage.

The cell was connected to a constant current source and a 10 ma/cm^2 forward current was passed through for 24 hours. Figure 3-b shows the I-V curve after the 24 hours. The current was then reversed. The voltage across the cell rapidly increased, was adjusted to 5 volts and applied for 24 hours. Figure 3-c shows the I-V curve after this biasing. The process appears to be reversible.

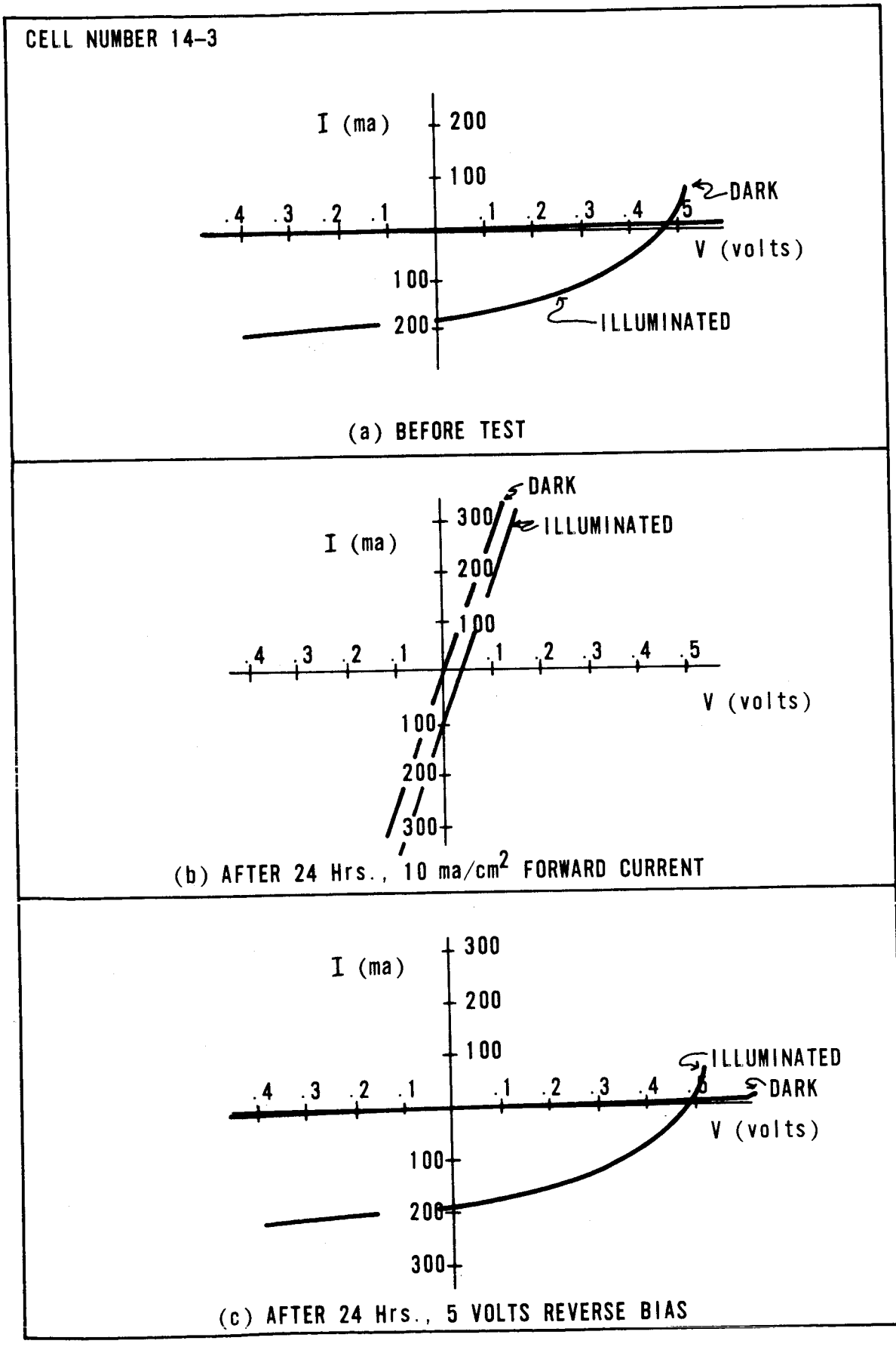

Fig. 3 REVERSIBLE CHANGES DUE TO APPLIED BIAS

During this test, another effect was noted. If the forward bias of a cell was removed after an extended time period and the cell was short circuited, a current would flow. In fact, power could be extracted from the cell. To study this further, the cell was biased in the forward direction and allowed to come to a steady state. It was then shorted and the current drawn recorded as a function of time. The time dependence appeared to be the sum of two decreasing exponentials.

Table I shows the pertinent data for two cells tested. Note the long time constants involved which indicate that relatively immobile charge carriers are involved. If this effect is the result of motion of ions in the space charge region, a few calculations are in order.

Assuming that the ions are singly charged, then the forward bias causes a drift and separation of the ions into a dipole layer. The negative ions are large compared to positive metal ions and, therefore, are considered essentially fixed. When the cell is shorted, it behaves as a condensor with stored charge. The current flowing can be related to the charge remaining by

$$I = \frac{Q}{\tau} = \text{current}$$

Q = Charge

τ = discharge time constant

Assume also that the charge Q is accumulated in two sheets (positive and negative) separated by a distance W in a material where the ion diffusion constant is D.

TABLE I - Bias Effects Data

	Forward Bias Voltage Time-Hours	I_{sc}** Amperes	τ_1 Minutes	τ_2 Minutes	Steady State Bias Voltage Volts	Steady State Bias Current Milliamperes	Extracted Charge μ Coul.	Open Circuit Voltage* Millivolts
Cell # 1 ↑	0.5	7×10^{-8}	2.8	9.2	.455	2.0	29	49
	72	6×10^{-8}	6.1	7.3	.45	2.7	29	13
	7	1.23×10^{-7}	2.1	6.4	.44	2.4	28.5	35
Cell # 1 ↓	16	1.41×10^{-7}	2.3	12.0	.49	10.0	91	30
	5	3.3×10^{-7}	2.1	10.8	.495	9.8	120	44
	0.5	5.3×10^{-7}	1.0	5.0	.52	9.0	78	95
Cell 1A ↑	3	8.2×10^{-8}	2.9	10.4	.475	10.0	36	0.2
	16	1.3×10^{-7}	3.0	22.0	.46	11.1	105	0.4
Cell 1A ↓	2	2.0×10^{-7}	1.6	10.6	.505	8.3	83	1.0

Electroformed Grid Cells

* Voltage appearing across cell immediately after removing bias

** Current generated by cell immediately after removing bias

Then

$$\tau = \frac{W^2}{D}$$

W = spacing of charge sheets

D = diffusion constant

By the Einstein relation

$$D = \frac{\mu kT}{q}$$

μ = ion mobility

k = Boltzmann's constant

T = absolute temperature

q = electronic charge

So that

$$\tau = W^2 q/\mu kT$$

$$\mu = W^2 q/\tau kT$$

Using the second set of data points with approximately equal time constants for the two ions, and assuming the charge separation is 10^{-4}cm

τ_1 = 6.1 minute

τ_2 = 7.3 minute

W = 10^{-4}cm

we find

μ_1 = 10^{-7}cm^2/volt second

μ_2 = 9×10^{-6}cm^2/volt second

For crystalline halides, the ionic mobilities at room temperature are on the order of 10^{-6} to 10^{-7} cm^2/volt sec., which is in good agreement with the measured values. Thus, it would appear that ionic motion can be the major cause of the long term hysteresis in the I-V data.

The effect of power extraction after application of forward bias is also recognized as persistent internal polarization, which was seen in CdS some time ago.[1]

Interface Materials

In order to make a more ohmic contact between the CdS and the substrate, several materials are being investigated as interface materials. In most cases, the materials have been applied by sputtering or electroplating.

In the first quarterly report[2] it was reported that of the metals investigated; namely, gold, silver, zinc, copper, silver appeared to be the best material.

Since then several cells have been made using sputtered silver interface layers of less than 0.5 mils. In the majority of cases, the cells with the silver interface have yielded slightly higher short circuit currents than the control cells (without the silver). This interface has been successful enough that with the approval of the contract monitor a small quantity of the cells produced on the pilot line will be made on silver coated molybdenum. The silver will also provide a solderable surface on the molybdenum tab.

More specific results follow.

Evaporations were attempted on galvanized metal. However, the CdS popped off the substrate before it could be removed from the vacuum chamber. The zinc should have provided an inexpensive, good ohmic contact to the CdS. The thermal expansion was too large to retain the CdS.

Some evaporations have been made on 2 mil 1010 sheet steel both silver coated and with roughened surface. Considerable curling and evidence of an appreciable series resistance in the final cells was noted.

Experiments with silver coated copper indicated that this combination would be useable. There is some curling but it is not excessive. Cells made on the copper-silver substrate have been comparable to those made on molybdenum. Careful control is necesary in many instances or the silver may separate from the copper. Due to the extra handling problems associated with the copper, molybdenum will continue to be used.

The new nickel plating process reported under Solderable Contacts has been used to provide an interface material on the molybdenum. No immediate advantage was apparent.

In the past titanium has been an attractive substrate material both because of its lower density and thermal expansion coefficient. However, cells made on titanium show a rapid deterioration after a period of about two weeks of apparent stability. Upon examination a darkening was found at the surface of the titanium when the CdS film was stripped.

During this quarter, cells were fabricated on sandblasted or sandblasted and silver (sputtered) coated titanium. All of these substrates were glow-discharged prior to CdS evaporation. The unexpected increase in stability in the titanium substrate cells prompted removal of some CdS for examination of the CdS-Ti interface. After one and two months, no discoloration was visible. So as it has not been determined whether the surface treatment or the glow discharge is the important factor determining the improved condition. Additional cells will be produced.

CdS Closed Space Vapor Transport Films

The formation of CdS thin films in the thickness range of 10 μ to 40 μ by a closed space vapor transport method has continued. High material utilization, predictable resistivity, reproducibility, soft pliable cell, larger grains, lower operating temperatures, cleaner vacuum system, and the need for only moderate vacuum pressure equipment are benefits accruing from this approach.

Fixture

The 700°C powder temperature reported last quarter(2) produced films somewhat too thin for convenient cell formation plus a longer than desired deposition time. The temperature range of 700°C to 750°C was investigated.

The increase in temperature caused an area in the boat to be hotter. This in turn caused the powder to transport more rapidly from the hot area and after a short time produced temperature gradients in the heater itself. The resulting film displayed an identical "hot area" as a circle of slightly thicker film of different texture but poor adhesion. A change in the heater sample holder was indicated. The flat heater sheet was made 3 inches wider, but the powder holder was kept unchanged. This cut down the cooling of the edges of the powder holder. See Figure 4.

The change proved beneficial since a 3 x 3 inch film can be made with uniform heat and thickness at the present operating temperature.

Film Development

After measuring the resistivity of the first several films

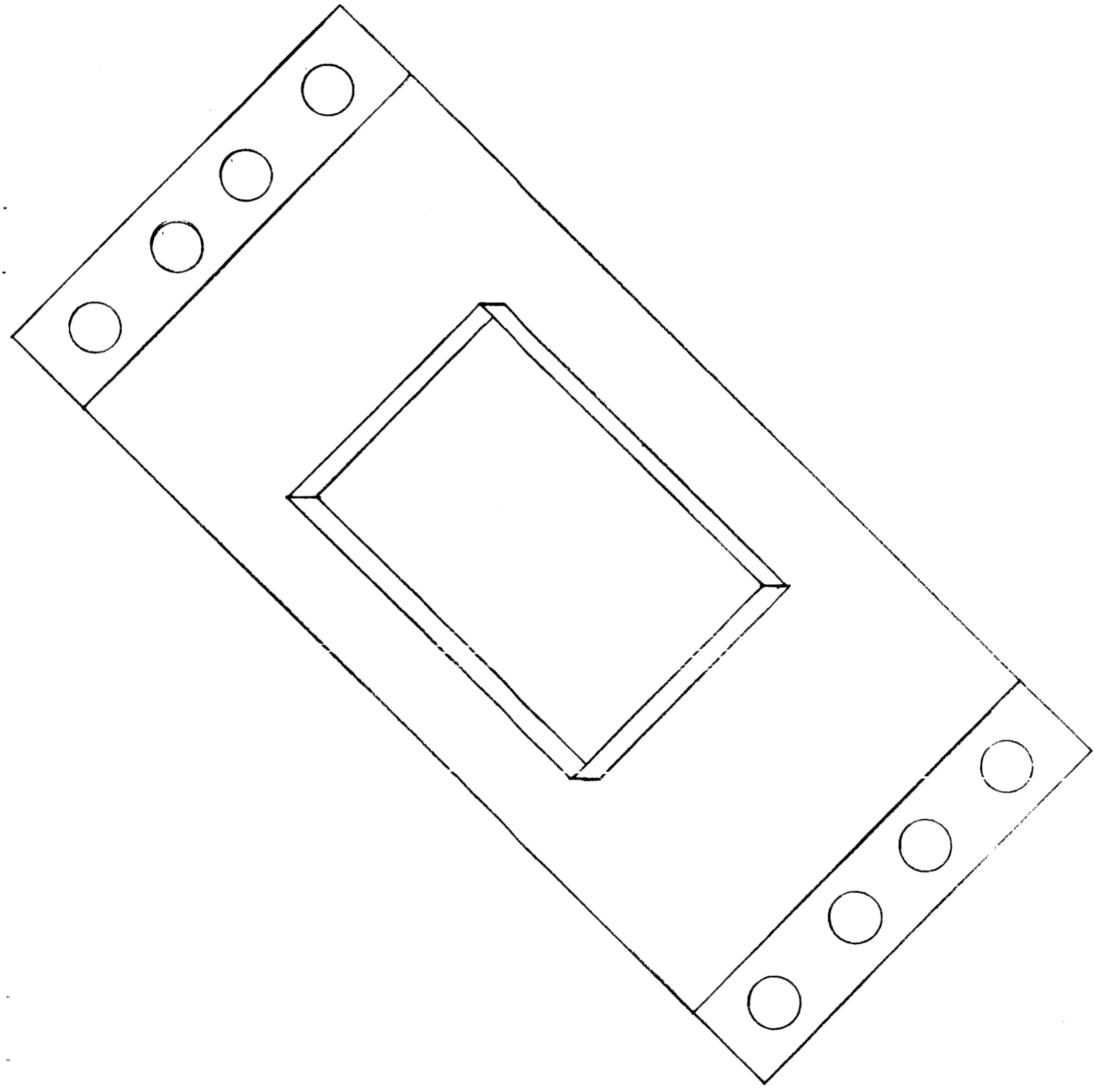

Vapor Transport Heater Holder

Figure 4

made with the new boat, it was found that individually prepared, consecutive, films varied from 100Ω-cm to 1 x 10^4Ω-cm although produced under the same conditions from the same batch of powder. Therefore, a change in the mixing technique was required to provide films with good reproducibility under the same run conditions.

Several "dummy" runs were made to determine the change in the temperature and power requirements while using 0, 0.6, and 3.0 gms. of charge in the boat. The substrate temperature was also measured in each run to determine the gradient. From the data obtained it was seen that the temperature gradient was 73$\pm$ 10°C for all runs. No separate substrate heater was used; however, a reflector was installed over the substrate. The powder-heater temperature was measured with a thermocouple welded to the heater. This provided the most consistent results.

Over fifty runs were made varying the heater temperature and amounts of powder in the boat. The primary objective was to produce a thicker film in less time than reported previously.

It was found that at temperatures below 700°C the rate of transport was too slow (approximately 2 microns/hr.). At temperatures over 750°C the rate was too high. The films had very poor adhesion to substrate. After a series of runs, a heater temperature of 730°C was found to be the best operating temperature for a film 10 to 12μ thick. The time required for the thickness was 30 minutes. However, it was noted that when an amount of powder less than 6 gms. was placed in the boat, the powder would transport very rapidly in certain areas of the

boat. This seemed to be the cause of the "hot spot" in the films reported above. Ten (10) grams of powder has been established as the proper charge for this boat. The depth of this powder is approximately 1/16 inches.

Several CdS powders were utilized to determine whether one type transported better than another. A brief outline of the results is given below:

Powder	Results
General Electric Unsintered CdS - Lot #185	The time required for a thickness of 12 μ was at least 90 minutes. Film chipped off if temperature went over 700°C for 90 minutes.
Harshaw CdS - 93-6 sintered	Same as above
Harshaw CdS - 0-44-A (Large crystal size, Ave. ~ 20 μ)	Same as above
Harshaw CdS - This was sintered, then pulverized	Same as above
Sylvania Lot #625 AUW (Luminescent Chemicals)	Good adhesion at a higher temperature. Faster transport rate.
Sylvania Type - S-20 CdS	Best results to date. With this powder, good polycrystalline films from 20 to 30μ in thickness are made in 30 minutes.

It was also found that using an inert atmosphere, such as argon, was not necessary. Several runs were made using air at 1×10^{-3} mm Hg pressure and the transport rates were unaffected as compared to those made in argon. Therefore, argon is no longer used.

After fifty runs the heater holder was replaced because several cracks had developed. A white crust was discovered on the boat. Upon replacing this boat, the transport rate dropped markedly.

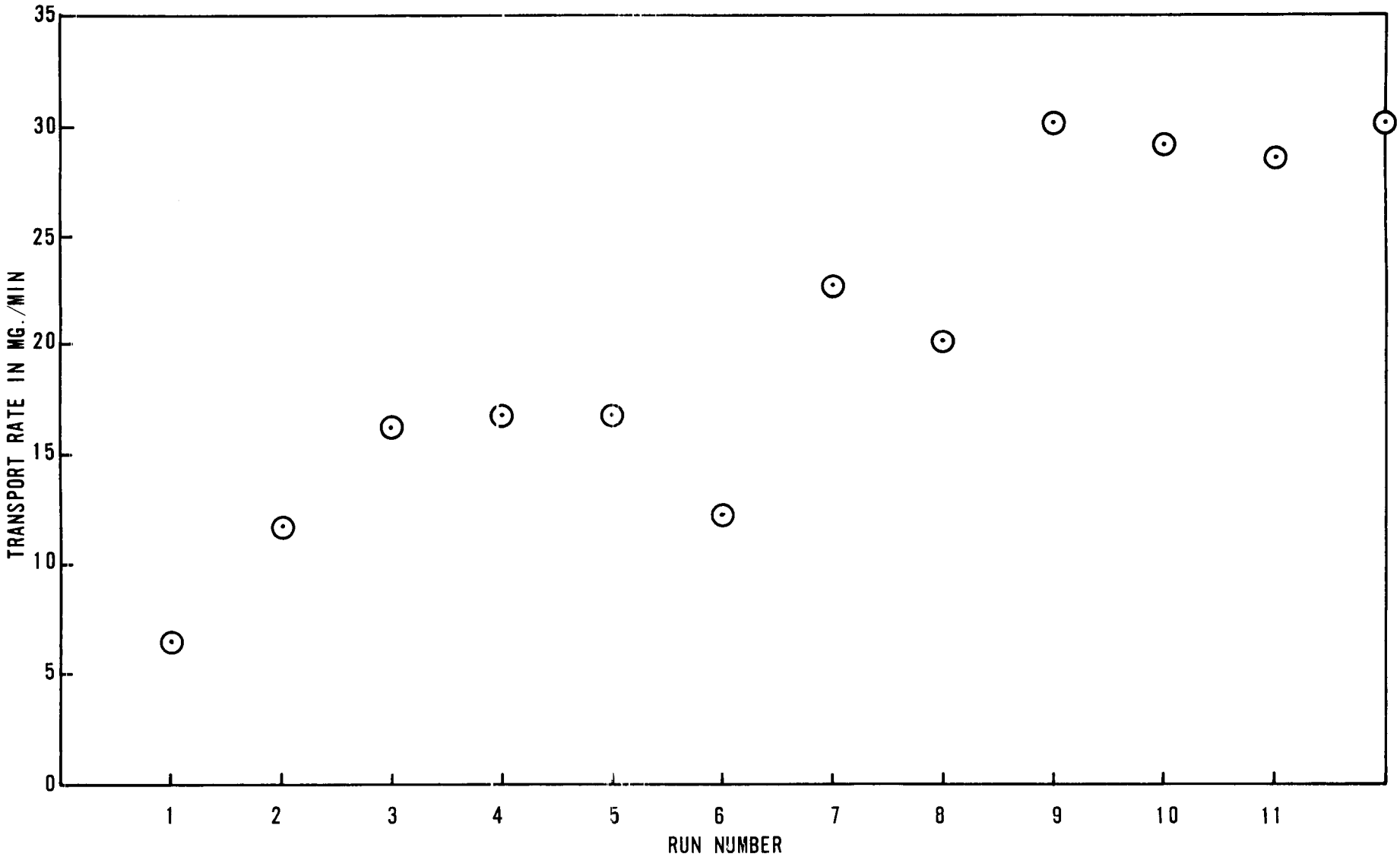

Fig. 5 TRANSPORT RATE Vs RUN NUMBER

The transport rate had been noticeably high during the last twelve runs with the old heater holder. Thus, in the following series of runs a plot of transport rate in mg per minute of CdS deposited on the substrate versus the successive run numbers. See Figure 5. It can be seen that as the white crust forms the transport rate increases. The crust has been removed and analyzed. It was found to contain a high concentration of tantalum. There has been no conclusion as to how this crust can increase the transport rate. Nevertheless, these CdS films are being produced in 30 minutes to a thickness of 20 to 30 microns. The crystal size is approximately 10 microns.

Cell Fabrication

Vapor transport films are being made into photovoltaic cells. Experiments with barrier formation and etchings are in progress to determine the most desirable process for this type of film. Its nature is such that modifications in procedure are needed.

Thicker films are necessary to enable the various experiments to be performed without fear of "shorting" through it. It is noted that to date there is no evidence of "shorting" from the barrier layer to substrate due to film pin-holes.

The films reported had resistivities below 100 Ω-cm. The first set of data were made after barrier formation. However, the next set was made two days later indicating that after heating a period of time is needed before the state of quasi-equilibrium is reached. Only a few cells have been laminated. These cells have not provided a high output efficiency and they represent only a small portion of the new films.

Following are typical data from the I-V curves of several cells produced from vapor transport films.

		Initial Readings		Two Days Later	
No.	t (microns)	j (ma/cm^2)	Voc (volts)	j (ma/cm^2)	Voc (volts)
V-100-1	21	5.6	0.42	6.4	0.43
V-100-2	21	3.3	0.35	6.7	0.40
V-100-3	21	6.7	0.42	8.3	0.40
V-100-4	21	6.0	0.38	5.8	0.44
V-100-1	24	2.2	0.40	5.5	0.44
V-102-4	24	6.0	0.42	6.3	0.44
V-103-1	21	1.1	0.30	5.8	0.40
V-103-3	21	4.4	0.38	6.7	0.40
V-103-4	21	5.5	0.40	6.4	0.43
V-104-4	23	6.7	0.41	6.4	0.42
V-105-3	22	6.7	0.39	6.7	0.41

The spectral response has been measured for a typical vapor transport type cell. Figure 6 is a plot of the data. A slight difference appears when compared with the evaporated type cell. More measurements will be made to determine whether a significant difference actually exists.

CdS Surface Treatments

A pre-treatment of the CdS surface prior to the barrier layer formation plays a crucial role in the ultimate performance of the cell. The parameter mostly affected is the short circuit current. The reason for this dependence is that the short circuit current directly depends on the thickness of the barrier layer and the number of n-type impurities in it. Both of these depend on the nature of the CdS into which the p-type layer is formed.

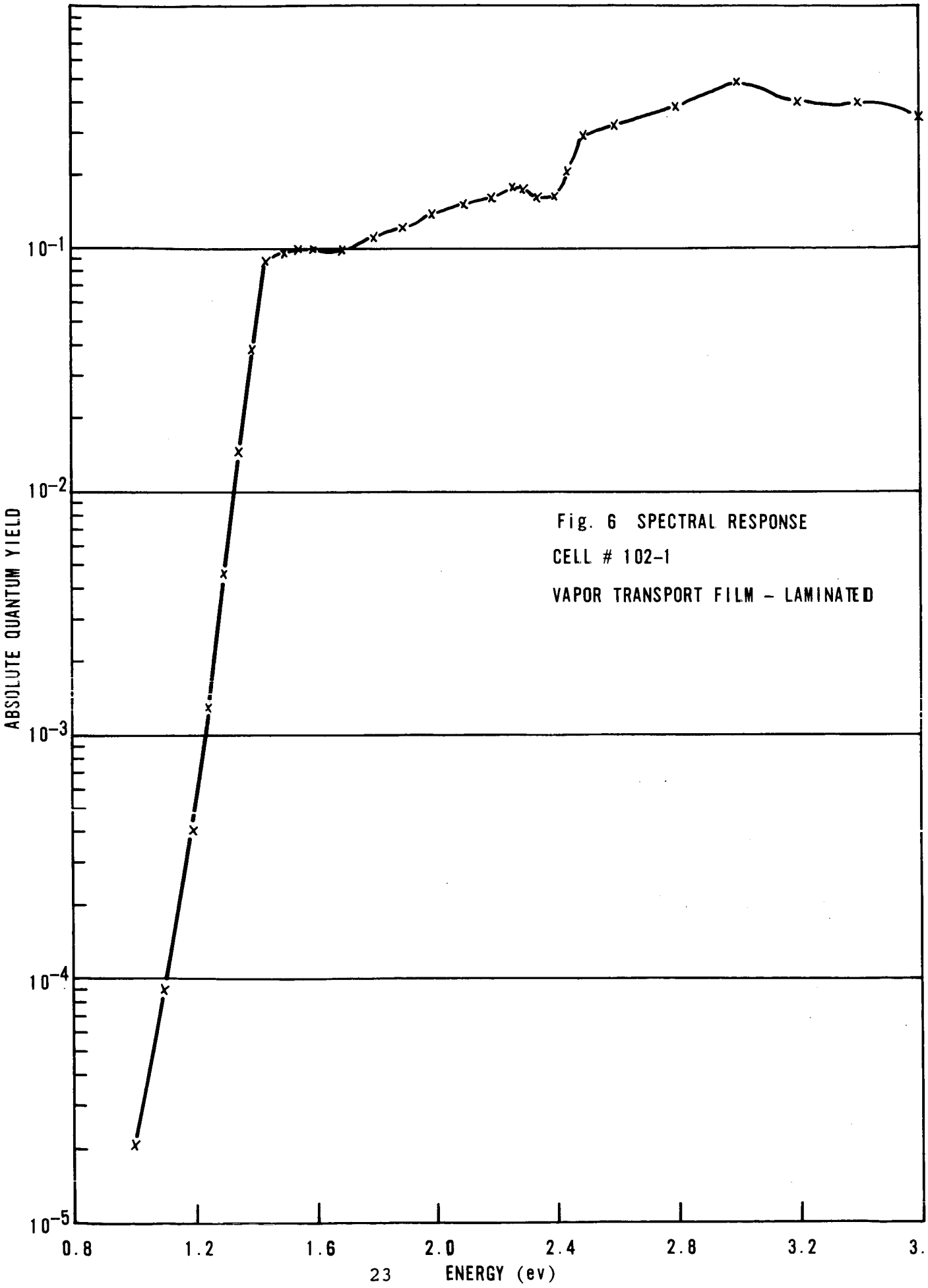

Fig. 6 SPECTRAL RESPONSE
CELL # 102-1
VAPOR TRANSPORT FILM - LAMINATED

An acid etch of the CdS surface can either reduce the current output to a value as low as 0.1 ma/cm^2 or enhance it by 20-40% over the current value achieved by making a cell with untreated CdS surface.

Surfaces etched with a mixture of six parts glacial acetic acid, three parts fuming nitric acid and three parts distilled water gave very low current output if any at all. Excess sulfur was left behind on the surface of the CdS after the etching and the subsequent rinsing.

The results of etching the CdS surfaces with H_2SO_4 or HCl are comparable when the performance of the cells made is used as the criterion. The rate of etching is not linear with time. During the first 30 seconds there is considerable etching activity after which etching slows down. Table II shows the drop in weight loss after each of the six 20 second immersions. Etching rates were determined by calculating from the weight loss data.

Etching a CdS film for 60-80 seconds in concentrated H_2SO_4 or for 30 seconds in 1:1 HCl:H_2O is sufficient to provide a CdS surface which will give a cell of optimum performance. A shorter etch does not remove all the undesirable impurities from the CdS surface and a longer one causes deep etching along the grain boundaries of the crystallites. Such deep etching prepares the ground for a spread-out junction between the n-type CdS and p-type Copper Sulfide and ultimately causes shorting paths.

The current output of cells made from etched films is on the average 20 - 40% higher than the output of cells made of

Table II

CdS Weight Loss During Etching

Immersion Number	Weight Loss For Each 20 Sec. Immersion Sample Number			
	1	2	3	4
1	1.8mg	2.0mg	2.2mg	2.0mg
2	2.0mg	1.8mg	1.9mg	1.9mg
3	1.5mg	1.3mg	1.2mg	1.3mg
4	1.1mg	1.0mg	1.3mg	1.1mg
5	0.6mg	0.5mg	0.7mg	0.4mg
6	0.3mg	0.4mg	0.4mg	0.4mg

Etchant: Concentrated H_2SO_4

Etched Area = $4cm^2$

All samples were from same CdS film

films with unetched surfaces. Cells were also made from films, the surfaces of which were lapped with 600 and 1000 grits and polished with Linde A polish, and finally from films which were lapped and polished as above and then etched for short intervals of time. Representative data can be seen in Table III.

All these preparations of the film prior to the barrier layer formation demonstrated that the nature of the surface does indeed play an important role in the output of the cell. However, from the performance point of view, the maximum output is achieved by etching the films in concentrated H_2SO_4 or solutions of HCl and distilled H_2O.

TABLE III

REPRESENTATIVE DATA OF CELLS MADE FROM FILMS WHOSE SURFACES HAVE BEEN VARIOUSLY TESTED PRIOR TO THE BARRIER LAYER FORMATION

Sample		I_{sc}	V_{oc}	Area
1	(Not etched)	50 ma	.43v	4.0 cm^2
2	(" ")	52 ma	.43v	4.0 cm^2
25	(Etched in acetic acid, nitric acid, distilled H_2O 6:3:3)	0.2 ma	.10v	4.0 cm^2
26	(Same as sample 25)	0.2 ma	.30v	4.0 cm^2
7	(Etched in conc. H_2SO_4 for 30 Sec.)	59 ma	.43v	4.0 cm^2
8	(" " " " " " ")	60 ma	.42v	4.0 cm^2
15	(Etched in conc. H_2SO_4 for 70 Sec.)	80 ma	.43v	4.0 cm^2
16	" " " " " " ")	70 ma	.43v	4.0 cm^2
21	(Etched in 1:1 HCl:H_2O for 30 Sec.)	68 ma	.44v	4.0 cm^2
22	(" " " " " " "	65 ma	.44v	4.0 cm^2
27	(Lapped with 600 Grit)	10 ma	.39v	4.0 cm^2
28	(" " " ")	12 ma	.41v	4.0 cm^2
29	(Lapped with 1000 Grit)	15 ma	.39v	4.0 cm^2
30	(" " " ")	13 ma	.41v	4.0 cm^2
31	(Lapped with 600 & Etched)	18 ma	.41v	4.0 cm^2
32	(" " " " ")	16 ma	.42v	4.0 cm^2
33	(Lapped with 1000 & Etched)	34 ma	.46v	4.0 cm^2
34	(" " " " ")	35 ma	.45v	4.0 cm^2
35	(Polished with Linde A)	38 ma	.46v	4.0 cm^2
36	(Polished & etched)	42 ma	.44v	4.0 cm^2

Non-Aqueous Barrier Formation Solutions

Water in the liquid or gaseous state is known to be detrimental to the CdS thin film cell. Fabrication of a water sensitive device in water media would appear to prevent attainment of maximum cell efficiency.

If water does react in a detrimental manner during the barrier formation as it does after cell fabrication, then removal of water should be beneficial.

Solutions of CuCl were prepared using formamide and ethylene glycol as solvents. These solvents are not completely non-aqueous and may have as much as 1% water present. Formamide was chosen because of its great similarity to water, particularly with respect to solvent properties.

For the formamide investigation, 4 gram/liter of CuCl was added. The CuCl turned yellow immediately and settled. The supernatant liquid remained colorless. Solution was heated to 70°C causing much of the solids to dissolve. Several etched CdS films were immersed, rinsed, heated at 250°C and tested. Results appear in Table IV. The same technique was followed with the ethylene glycol. No indication of solvent reaction was noted when the solution was prepared.

As can be seen from the table, cells can be prepared by this approach but nothing spectacular is apparent.

The better cells, -2, -6, -14 were laminated. OCV was 0.48, 0.47, and 0.48V respectively; SCC was 17, 9, and 59 respectively; and efficiencies were 0.7, 0.3, and 2.0% respectively. The latter barrier was slate gray.

Table IV

CdS Cells Prepared In Non-Aqueous Media

Film No.	Etched	Solvent	Temperature	Immersion Time	OCV	SCC	Remarks
113-3-1	X	Formamide	70°C	5 sec.	.42V	12mA	
113-3-2		Formamide	70°C	5 sec.	.47V	12mA	
113-2-11	X	Formamide	70°C	20 sec.	.31V	12mA	
113-2-12		Formamide	70°C	20 sec.			Open
108-3-13	X	Formamide	70°C	50 sec.	.40V	19mA	
108-3-14		Formamide	70°C	50 sec.	.49	43mA	
108-2-15	X	Formamide	90°C	20 sec.	.39	10mA	
108-2-16		Formamide	70°C	20 sec.	.40	7mA	
113-3-3	X	Ethylene Glycol	70°C	5 sec.			Open
113-3-4		Ethylene Glycol	70°C	5 sec.			Open
113-2-5	X	Ethylene Glycol	70°C	20 sec.			Open
113-2-6		Ethylene Glycol	70°C	20 sec.	.45	6mA	
108-3-7	X	Ethylene Glycol	70°C	50 sec.			Open
108-3-8		Ethylene Glycol	70°C	50 sec.	.46	5mA	
108-2-9	X	Ethylene Glycol	90°C	20 sec.			Open
108-2-10		Ethylene Glycol	90°C	20 sec.	.47	7mA	

Cell size was 1-1/4" x 1-1/4" for all experiments

Vapor Transport of Cu_2S

During this quarter data has been taken on the vapor transport of Cu_2S and CdS to determine the feasibility of vapor depositing films of Cu_2S onto CdS or vice-versa.

Two small two-zone furnaces were assembled by winding nichrome ribbon on quartz tubing which was then slid inside larger quartz tubing to reduce radiation heat loss. The larger diameter quartz tubing was then wrapped with asbestos over the hot zone. Associated power supplies and controllers independently controlled the temperature of each zone using a C/A thermocouple inside the smaller diameter quartz tubing. Temperatures could be maintained as high as 1100°C.

Varying amounts of Cu_2S (prepared by passing H_2S over semiconductor grade Cu at 800°C) and I_2 were sealed into small (5mm ID x 6") evacuated quartz tubes. The tubes were then placed in the two-zone furnace with approximately 1" of tube in the cold zone.

The transport velocity was computed from the visually observed change in size of the charge. If we assume that material is transported at a rate proportional to the exposed surface area, or $V(gms/sec) = k\ A(cm^2)$, then k is characteristic of the material and the two temperatures. Qualitative data taken on Cu_2S supports this assumption. The data indicates that,

a. Cu_2S does not transport by evaporation for

$$T\ (\text{feed pile}) = 1050°C$$

$$T\ (\text{cold zone}) = 600°C$$

although considerable crystal growth takes place on the feed pile.

b. Transport of Cu_2S takes place in the presence of iodine vapor for T (feed pile) $\geq$ 1000°C. The dependence of transport on the iodine density is given in Figure 7.

c. The crystal size of the transported Cu_2S depends on the temperature.

d. For T (cold zone) $\geq$ 300°C, the transported material does not recombine to form Cu_2S but deposits as CuI and S.

e. Transported Cu_2S deposits preferentially on Mo, forming large crystals.

Several runs were made to examine the transport of CdS in the small sealed tubes. The results indicate that

a. CdS transports very slowly by evaporation at

T (feed pile) = 700°C,

T (cold zone) = 600°C,

The condensate consists of needles, approximately 1mm x 0.01mm.

b. CdS transports very rapidly in the presence of iodine vapor at the same temperatures. The condensate consists of several crystals which exhibit the same shape as natural crystals of Greenockite.

c. A CdS crystal with a chemiplated surface transported rapidly at the same temperatures. The condensate consisted of deep red crystals showing the shape observed for the transport of CdS. The feed pile residue was a black crystal with an octahedral shape indicating that it was Cu_2S.

d. For T (cold zone) $\geq$ 300°C, the transported material does not recombine to form CdS but deposits as CdI_2 and S.

The observations taken on the transport of Cu_2S suggests that the close spaced transport technique described by

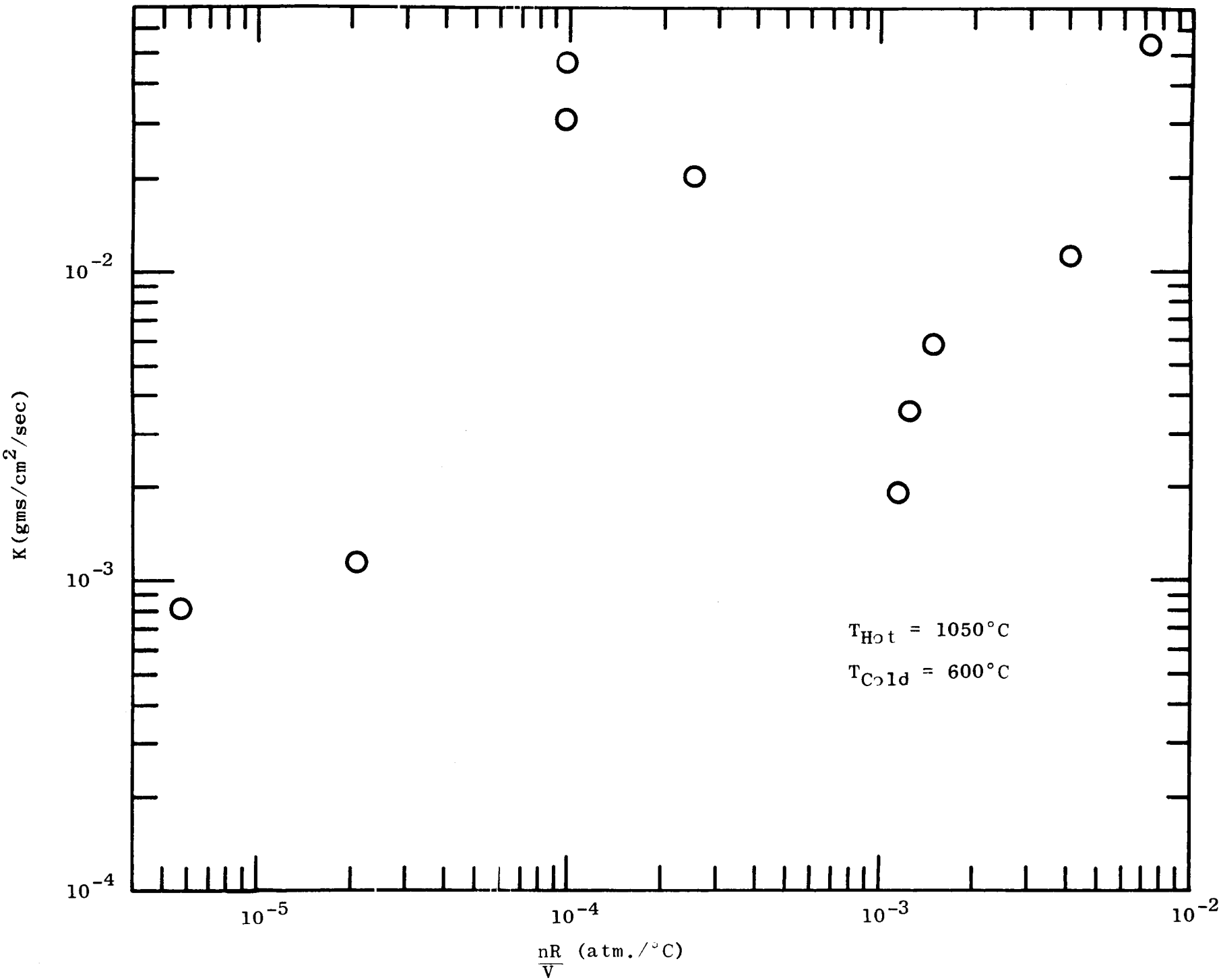

Figure 7 Transport Velocity of Cu_2S with Iodine

Nicoll[3] would not be suitable for the preparation of large films of Cu_2S. A more appropriate system would be an open tube utilizing a flowing gas.

Early success with respect to thin film solar cells is not expected so this phase of the program has been curtailed.

Collector Grids

Electrodeposited Grids

Yield

The improvements in electroplating techniques noted in a previous report[2] have continued toward increased yields. Two advantages can be given for this type of grid; (1) very high reliability and stability, and (2) low material costs. Electroformed grids range from $2 to $4 per 3" x 3" whereas the electrodeposited cost about 30 cents. The overall yield based on 106 samples is 81%, as shown on the bar graph in Figure 8. (This compares with a yield figure of 67% noted during the first quarter.)

Last month 31 out of 33 cells were successfully gridded giving a yield of 93%. These results are based on efficiency before and after grid electroplating. One 1" x 1" cell with electroplated grid has an efficiency of 5.0%. This efficiency has been stable for two months. This will be submitted to NASA Project Manager for evaluation.

Plating Solutions

Cells plated in a high speed gold plating solution were compared with cells plated in the standard manner. No difference was noted in electrical characteristics even though the high

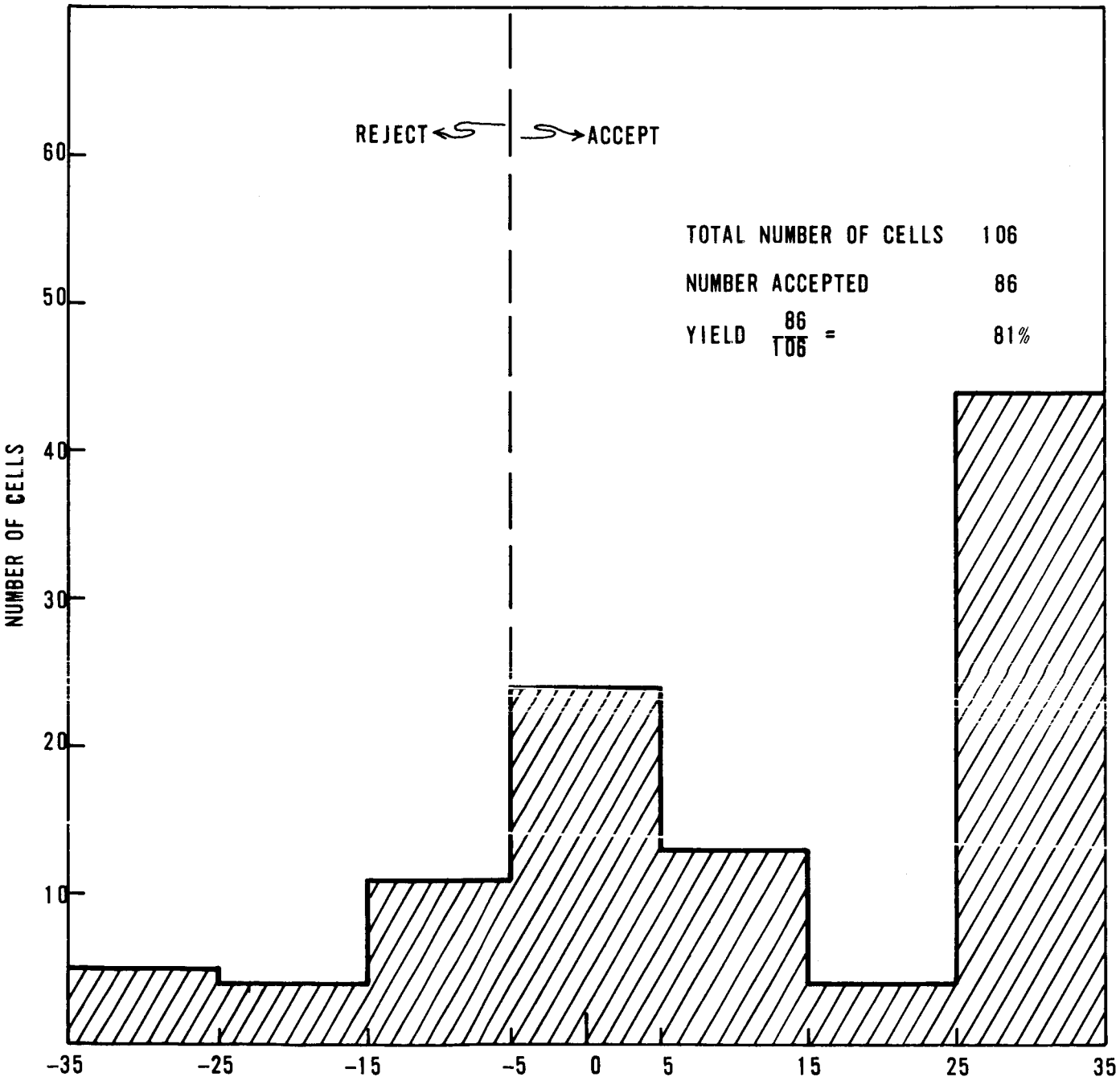

Fig.. 8 PERCENT CHANGE IN CELL EFF. DUE TO PLATING ELECTROPLATING YIELDS

speed process produced a thicker plate. This is due to the gold alloy in the standard procedure being more conductive than gold.

Lamination of Grid Electroplated Cells

On cells using the Buckbee-Mears electroformed mesh, and efficiency increase of about 25% is noted as a result of lamination. Some of this increase is due to better optical coupling as a result of the plastic film encapsulant and better electrical contact between the mesh and the p-layer. Other reasons for this increase are being considered as part of the cell model research effort. The major problem confronting grid electroplating is the absence of efficiency increase as a result of lamination. A study is under way to determine the difference between electroformed mesh cells and grid electroplated cells before and after lamination. I-V characteristics and spectral response measurements are being used as the principal means of comparison. As the first step in this investigation, the spectral response of an unlaminated cell before and after electroplating was measured. See Figure 9. Results to date show that the quantum yield on the grid electroplated cell is lower over the entire spectral response region. Additional data from several samples are necessary to confirm this result because the first samples used had a low quantum yield at energies above 2.5 eV.

Environmental Test on Grid Electroplated Cells

Figure 10 shows the results of vacuum environment on two sets of cells which are from different CdS evaporation runs, numbered 61 and R159. Data on both electroplated grid and

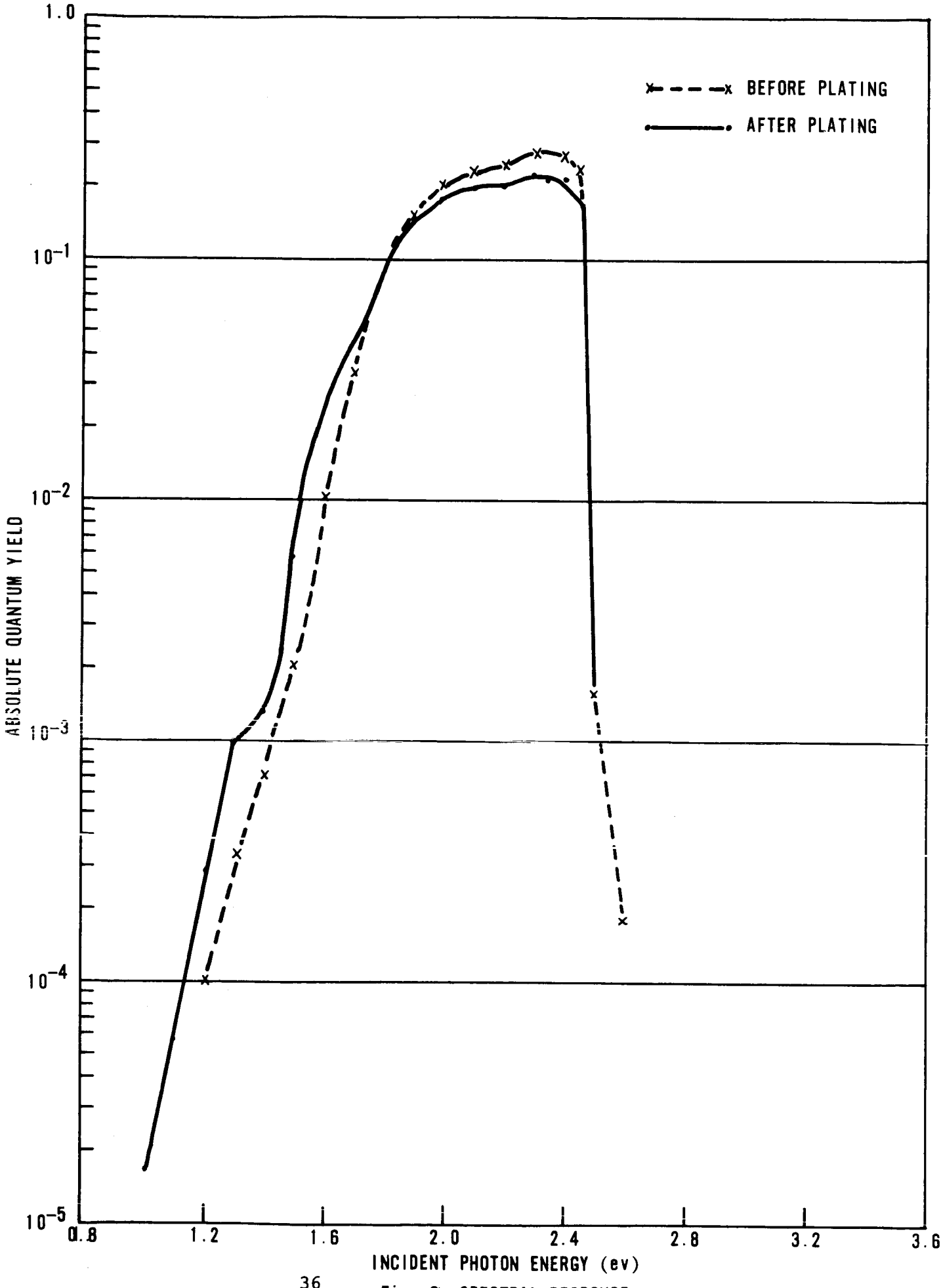

Fig. 9 SPECTRAL RESPONSE

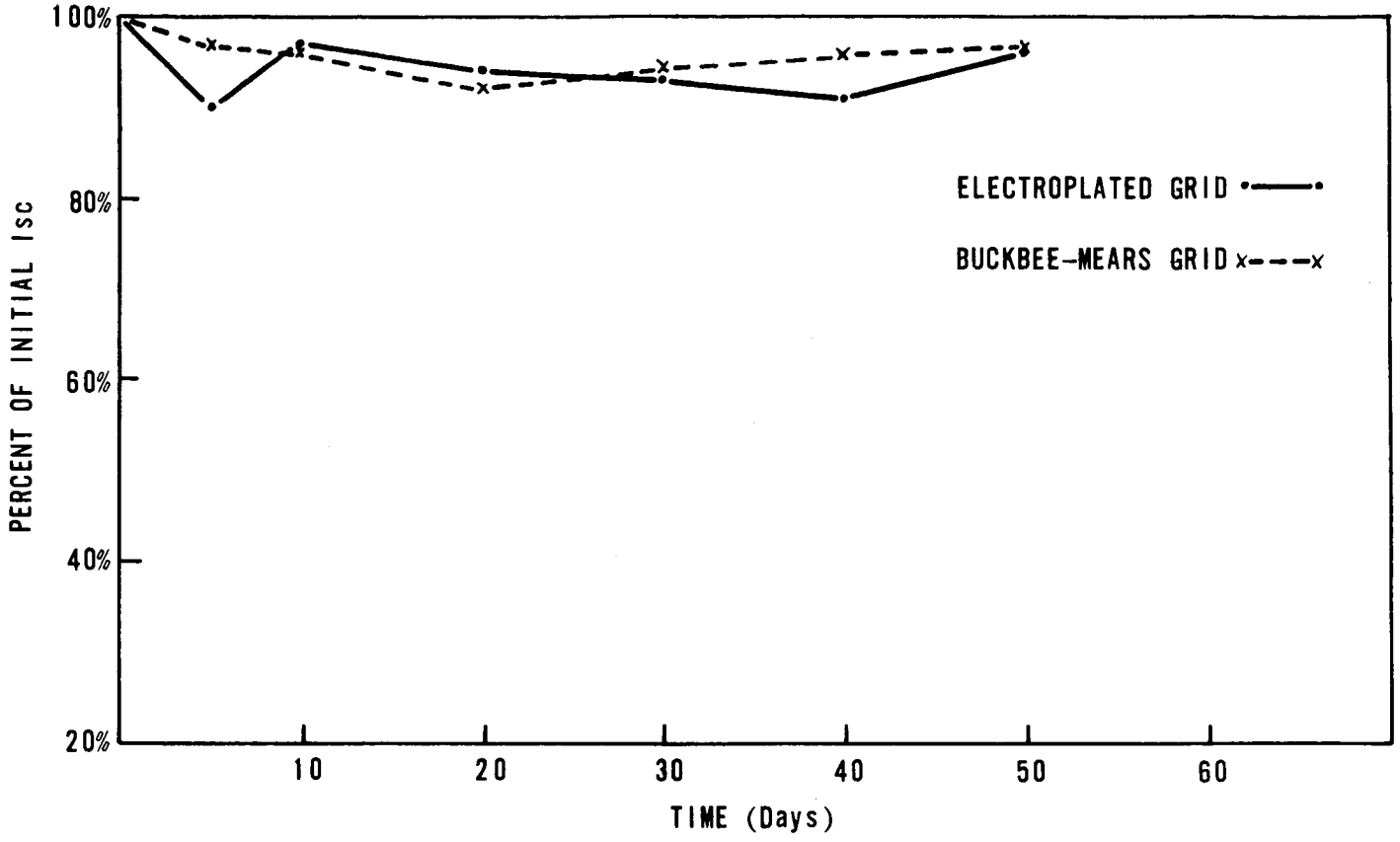

(a) RUN 61

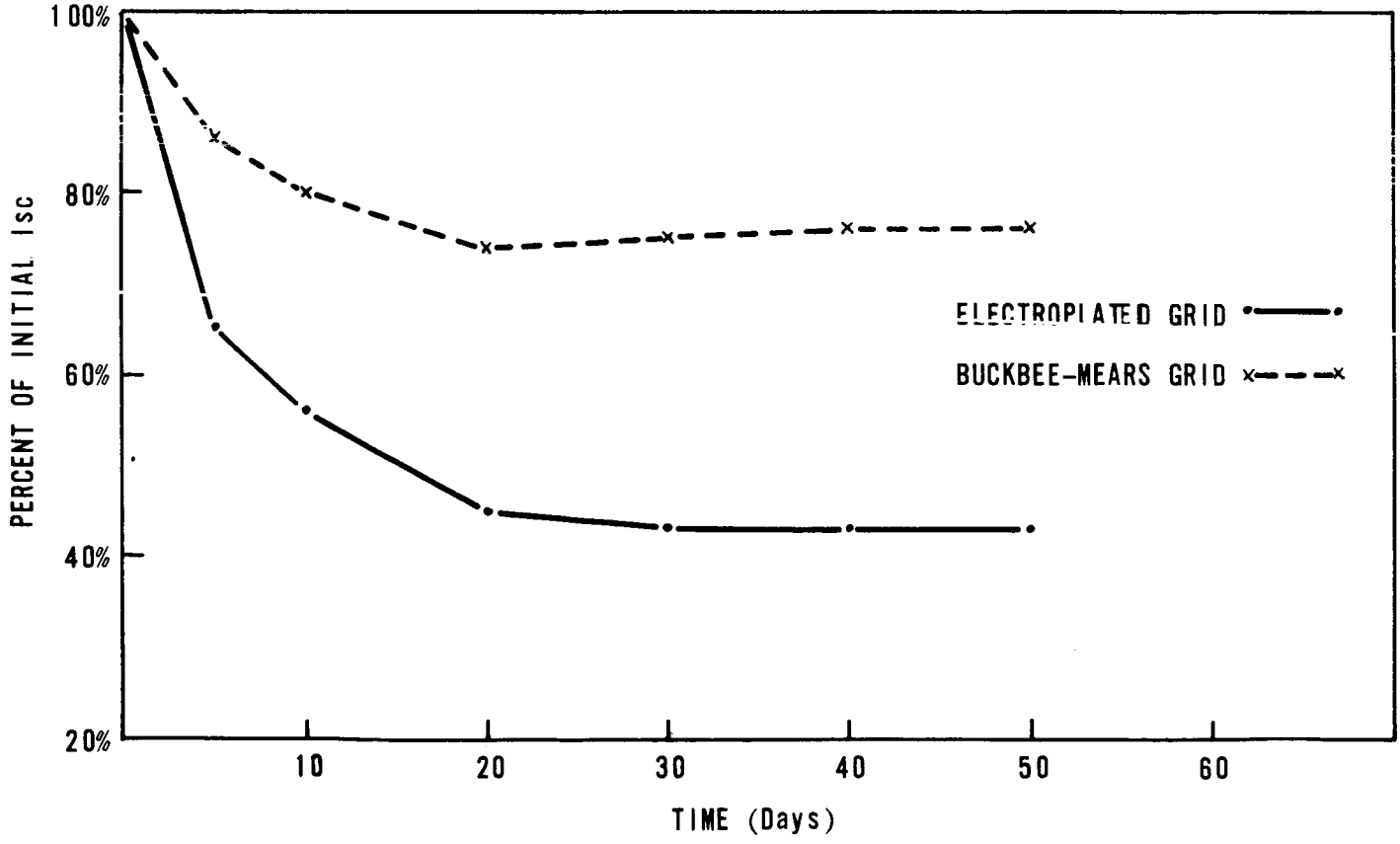

(b) RUN R159

Fig. 10 VACUUM ENVIRONMENTAL TESTS

Buckbee-Mears grid cells are reported for comparison. Figure 10A shows little degradation on cells from Run 61. The fluctuations are within the experimental error of the measurement. Figure 10B shows considerable degradation on both types of gridded cells. Since both groups from Run 61 did not degrade, it can be concluded that electroplating does not cause degradation after lamination even though the efficiency increase as a result of lamination is absent.

Electroformed Grids

New Method of Attachment

The collector grid design and the method of attachment to the cell has been a continuing problem. Several approaches to an acceptable solution have been followed with respect to selection of the grid material such as gold, silver, copper or nickel, and with respect to the method of attachment; i.e., lamination or electrodeposition.

Attachment of a metallic grid by the fusion of plastic during lamination provides the most efficient collection of current initially but does not remain attached over a long period of temperature cycling. The electrodeposited grid previously did not provide an initially high collection efficiency, but does provide a tenacious grid with very high reliability during thermal cycling for cells of 5% efficiency.

Although the efficiencies reported for the electrodeposited grid have reached the 5% level and that the total amount of materials per cell is less than any other workable method, it

is also desired to provide a more rapid method of grid attachment. A Harshaw Company funded project has found that electroformed gold and other metals could be compression-bonded to the cell surface with varying degrees of success. Because of the success and simplicity of the procedure, it was felt that the compression bonding approach was worthy of further investigation on this contract.

The primary objectives are (1) Ease and rapidity of attachment, (2) Stability and reliability, particularly with respect to thermal cycling, (3) Lower labor cost, (4) Cells with open face, and (5) Numerous new methods of encapsulation.

The compression bonding procedure is essentially the positioning of the desired grid material on the face of the cell, placing the cell between two sheets of shim stock steel or other suitable stock, and then applying the heat and pressure in the range of 3000 p.s.i. simultaneously.

Bonding of gold grid to the CdS cell was quite successful with this method and samples are being prepared for submission to NASA for temperature cycling tests. Other metal grids have been used and have been found to bond to a lessor degree. Further experimentation is expected to provide cells with the cheaper metal collectors such as copper and nickel.

Lamination

There are strong indications that no encapsulation with plastics is required for this procedure. Thinner, uncovered cells are possible provided covers are not needed to exclude moisture and to provide protection from 0.5 MeV protons.

Samples are being prepared for submission to NASA, Lewis Research Center.

Substrate Milling

Electrochemical Milling

Experiments involving electroetching or milling of the substrates have been concluded. Cells fabricated on 2 mil molybdenum can be milled electrochemically after lamination. The exposed back of the cell is made anodic after immersion in the solution as per instructions given in the First Quarterly Report. Cells can be produced with high watts per pound values by this procedure. Care must be exercised in the selection of the shape cathode and the distance of the cathode from the cell otherwise "edge-effect" will cause a rapid attack at the cell's edges. The attack can cause complete removal of the substrate leaving the CdS layer exposed. An extreme case would be formation of a small hole completely through the cell unit.

Chemical Spray Milling

A commercial spray etcher has shown success. Mechanical and electrically operative samples of CdS cells (.002" substrates) were spray-etched to a uniform thickness of 0.0005". Etching was done on a double-sided, horizontal spray etcher using H_2SO_4, HNO_3, and H_2O in 1:1:1:5 ratio. Etch time was 17 seconds and maximum temperature during etching was 130°F. Both electrically operative cells (S62B and N132C) did not degrade as a result of this spray etching but remained unchanged. This method of molybdenum removal to reduce overall cell weight is more reliable than the chemical immersion-etch with HNO_3 and the electrochemical etch with KOH. Any future commercial requirement for very thin CdS cell substrates can utilize the commercially

available spray etching equipment.

Solderable Contacts to Molybdenum

A process has been developed by a subsidiary of The Harshaw Chemical Company that can be employed in cell fabrication. By use of this process, nickel coatings (thickness in the thousand Å range) can be plated onto the molybdenum substrate. This eliminates the need for a two mil thick nickel interface for welding leads to the molybdenum. Furthermore, this coating is extremely adherent and allows leads to be soldered or welded directly to the substrate. Wires soldered to the molybdenum broke before the solder joint. This method is expected to produce increased contact reliability. This knowledge is being applied in the fabrication of NASA cells. The nickel plate can be applied at any point in the cell process without damage to the cell.

Another advance in plating was announced recently by The General Electric Company. They discovered that molybdenum treated with peroxide can be plated with gold or other metals. The coating is said to be tough and adherent.

Pilot Line

During this quarter sixty-four 3" x 3" cells were fabricated on the pilot line. The average efficiency was 3.2%. The highest efficiency was 4.8%. All of these efficiencies were taken before lamination. Lamination should improve them.

Several of the films made during this quarter displayed I-V curves indicating a double diode. The cause was finally traced to a thin layer that formed on the substrate when the substrate heater was turned on prior to evaporation. Formation

of this film can be prevented by baking out the heater before the substrate is placed in the holder. This problem seems to have been occasioned, or at least made acute, when the substrate filament distance was shortened by 30%. This source-substrate distance has been returned to nine inches and the substrates are baked out before each run.

Several cells were supplied to Contract NAS3-6464 for various anti-reflective coatings during this period.

References

(1) H. Kallman and B. Rosenberg - Phys. Rev. 97 1596, (1955)

(2) First Quarterly Report - Contract NAS3-7631

(3) F. H. Nicoll, J. Electrochem Soc. 110 (11), 1165, (1963)

THE HARSHAW CHEMICAL COMPANY
CONTRACT NAS3-7631
DISTRIBUTION LIST

QUARTERLY AND FINAL REPORTS

National Aeronautics and Space Administration
Washington, D.C. 20546
Attention: Arvin H. Smith/RNW (2)
H. B. Finger/RP
Millie Ruda/AFSS-LD

National Aeronautics and Space Administration
Scientific and Technical Information Facility
P.O. Box 5700
Bethesda, Maryland 20546
Attention: NASA Representative (5 + 1 Reproducible)

National Aeronautics and Space Administration
Goddard Space Flight Center
Greenbelt, Maryland 20771
Attention: W. R. Cherry
M. Schach
B. Mermelstein, Code 672
J. W. Callaghan, Code 621
Librarian
P. H. Fang, Code 633

National Aeronautics and Space Administration
Lewis Research Center
21000 Brookpark Road
Cleveland, Ohio 44135
Attention: John E. Dilley, M.S. 500-309
B. Lubarsky, M.S. 500-201
H. Shumaker, M.S. 500-201
R. L. Cummings, M.S. 500-201
C. K. Swartz, M.S. 500-201 (3 + 1 Reproducible)
N. D. Sanders, M.S. 302-1
A. E. Potter, M.S. 302-1 (3)
C. S. Corcoran, M.S. 500-201
V. F. Hlavin, M.S. 3-14 (Final Only)
George Mandel, M.S. 5-1 (2)
Report Control Office
Technology Utilization Office, M.S. 3-19
Office of Reliability & Quality Assurance, M.S. 500-203

National Aeronautics & Space Administration
Langley Research Center
Langley Station
Hampton, Virginia 23365
Attention: W. C. Hulton
E. Rind

National Aeronautics & Space Administration
Electronic Research Center
Power Conditioning & Distribution Lab.
575 Technology Square
Cambridge, Massachusetts 02139

Jet Propulsion Laboratory
4800 Oak Grove Drive
Pasadena, California 91103
Attention: John V. Goldsmith
Don W. Ritchie

Institute for Defense Analysis
Connecticut Avenue, N.W.
Washington, D.C. 20546
Attention: R. Hamilton

Advanced Research Projects Agency
Department of Defense, Pentagon
Washington, D.C. 20546
Attention: Dr. C. Yost

Naval Research Laboratory
Department of the Navy
Washington, D.C. 20546
Attention: E. Broncato, Code 6464
M. Wotaw, Code 5170
Dr. V. Linnenbom, Code 7450
Dr. C. Klick, Code 6440

U.S. Army Signal Research and Development Laboratory
Fort Monmouth, New Jersey
Attention: Power Sources Branch

Air Force Cambridge Research Center
Air Research and Development Command
United States Air Force
Laurence G. Hanscom Field
Bedford, Massachusetts
Attention: Col. G. de Giacomo

Air Force Ballistic Missile Division
Air Force Unit Post Office
Los Angeles 45, California
Attention: Col. L. Norman, SSEM
Lt. Col. G. Austin, SSZAS
Lt. Col. A. Bush, SSZME
Capt. A. Johnson, SSZDT
Capt. W. Hoover, SSTRE

Office of the Chief of Engineers
Technical Development Branch
Washington, D.C.
Attention: James E. Melcoln/ENGMC-ED

Aeronautical Research Laboratories
Office of Aerospace Research, USAF
Wright-Patterson Air Force Base
Dayton, Ohio
Attention: Mr. D. C. Reynoles, ARX
Chief, Solid State Physics,
Research Lab.

Aeronautical Systems Division
Air Force Systems Command
United States Air Force
Wright-Patterson Air Force Base, Ohio
Attention: P. R. Betheand
Mrs. E. Tarrants/WWRNEM-1

Flight Vehicle Power Branch
Air Force Aero Propulsion Laboratory
Wright-Patterson Air Force Base, Ohio
Attention: Joe Wise/Code APIP-2

Flight Accessories Aeronautics Systems Division
Wright-Patterson Air Force Base
Dayton, Ohio
Attention: James L. Matice, ASRCM-22

Aerospace Corporation
P.O. Box 95085
Los Angeles 45, California
Attention: Dr. G. Hove
Dr. F. Mozer
V. J. Porfune
Dr. I. Spiro
Technical Library Documents
Group

Battelle Memorial Institute
505 King Avenue
Columbus, Ohio
Attention: L. W. Aukerman
R. E. Bowman
T. Shielladay

Bell and Howell Research Center
360 Sierre Madre Villa
Pasadena, California
Attention: Alan G. Richards

Bell Telephone Laboratories, Incorporated
Murray Hill, New Jersey
Attention: W. L. Brown
U. B. Thomas

Clevite Corporation
Electronic Research Division
540 East 105th Street
Cleveland, Ohio 44108
Attention: Fred A. Shirland
Dr. Hans Jaffe

The Eagle-Picher Company
Chemical and Material Division
Miami Research Laboratories
200 Ninth Avenue, N.E.
Miami, Oklahoma
Attention: John R. Musgrave

Energy Conversion, Incorporated
336 Main Street
Cambridge 42, Massachusetts
Attention: G. J. McCaul

General Electric Company
Electric Components Division
316 East Ninth Street
Owensboro, Kentucky
Attention: F. D. Dyer, Jr.

Heliotek Corporation
12500 Gladstone Avenue
Sylmar, California
Attention: Eugene Ralph

Hughes Aircraft Company
Aerospace Group, R & D Division
Culver City, California
Attention: C. A. Escoffery

International Rectifier Corporation
239 Kansas Street
El Segundo, California
Attention: Irwin Rubin

Leesona Moos Laboratories
90-28 VanWyck Expressway
Jamaica 18, New York
Attention: Stanley Wallack

Lockheed Missile and Space Division
3251 Hanover Street
Palo Alto, California
Attention: D. Marks, Dept. 5230

Material Research Corporation
Orangeburg, New York 10962
Attention: Vernon E. Adler

Martin Company
Orlando, Florida
Attention: W. A. Headley, Jr.

National Cash Register Company
Physical Research Department
Dayton 9, Ohio
Attention: R. R. Chamberlin

North American Aviation, Incorporated
Autonetics Division
Anaheim, California
Attention: R. R. August

Perkin-Elmer Company
Optical Coating Section
Norwalk, Connecticut
Attention: Jim Peardsley

Philco Corporation
Blue Bell, Pennsylvania
Attention: Mr. A. E. Mace

Physics Technology Laboratories, Inc.
7841 El Cajon Boulevard
La Mesa, California
Attention: W. E. Richards

RCA Laboratories
Radio Corporation of America
Princeton, New Jersey
Attention: P. Rappaport

Ryan Aeronautical Company
Lindbergh Field
San Diego, California 92112
Attention: K. D. Hawkins

Sandia Corporation
Albuquerque, New Mexico
Attention: F. Smits

Sylvania Electronic Products, Incorporated
Electron Tube Division
Emporium, Pennsylvania
Attention: Georgiana Larrabee, Librarian

Tyco Laboratories, Inc.
Bear Hill
Waltham 54, Massachusetts
Attention: A. I. Mlavsky

Union Carbide Corporation
Parma Research Center
Technical Information Services
P.O. Box 6116
Cleveland, Ohio 44101

Solid-State Electronics Laboratory
Stanford Electronics Laboratories
Stanford University
Stanford, California
Attention: Prof. G. L. Pearson

Westinghouse Electric Corporation
Research and Development Laboratories
Churchill Borough, Pennsylvania
Attention: H. G. Chang

Westinghouse Electric Corporation
Semiconductor Division
Youngwood, Pennsylvania
Attention: Don Gunther

Massachusetts Institute of Technology
Security Records Office
Room 14-0641
Cambridge 39, Massachusetts